Mine burial in the seabed of high-turbidity area (Belgian coastal zone) - findings from a first experiment*

Matthias Baeye[1], Michael Fettweis[2], Sebastien Legrand[2], Yves Dupont[3], Vera Van Lancker[2]

[1]*Department of Geology and Soil Science,*
Renard Centre of Marine Geology (RCMG), Ghent University,
Ghent 9000, Belgium

[2]*Management Unit of the North Sea Mathematical Models*
(MUMM), Royal Belgian Institute of Natural Sciences,
Brussels 1200, Belgium

[3]*Naval Logistics (DIRNAVLOG),*
Belgian Defence, Marine Basis,
Zeebrugge 8380, Belgium

*accepted for publication in Continental Shelf Research (Elsevier)

M. Baeye processed and interpreted the datasets, wrote the manuscript and made all figures (except for Fig. 6.14). Co-authors helped by reviewing the manuscript and/or providing the datasets. S. Legrand was responsible for the 3D model (OPTOS-BCZ) results.

Abstract

The seabed of the North Sea is covered with ammunition dating back from World Wars I and II. With increasing human interference (e.g. fisheries, aggregate extraction, harbour related activities), it forms a threat to the safety at sea. In this study, test mines were deployed on a sandy seabed for three months to investigate mine burial processes as a function of hydrodynamic and meteorological conditions. The mine experiment was conducted in a shallow (9 m), macrotidal environment characterized by highly turbid waters (yearly and depth-averaged suspended particulate matter concentration of 100 mg l^{-1}). Results showed some variability of the overall mine burial, which corresponded with scouring processes induced by a (sub-) tidal forcing mechanism. The main burial events however were linked to storm-related scouring processes, and subsequent mine roll into the resulting pit. Two storms affecting the mines during the 3-month experiment resulted in enduring increases in burial volume to 60% and 80%, respectively. More cyclic and ephemeral burial and exposure events appear to be linked to the local hydrodynamic regime. During slack tides, suspended sediment settles on the seabed, increasing the burial volume. In between slack tides, sediment is re-suspended, decreasing the burial volume. The temporal pattern of this never reported burial mechanism, as measured optically, mimics the cyclicity of the suspended sediment concentration as recorded by ultrasonic signals at a nearby benthic observatory. Given the similarity in response signals at the two sites, we hypothesize that the formation of high-concentrated mud suspensions (HCMS) is a mechanism causing short-term burial and exposure of mines. This short-term burial and exposure increase the chance that mines are 'missed' during tracking surveys. Test mines contribute to our understanding of the settling and erosion of HCMS, and thus shed a light on generic sedimentary processes.

Keywords: Mine burial experiment; scouring; suspended particulate matter; high-concentrated mud suspension; slack tides

6.1. *Introduction*

World War I and II-era explosives are scattered over the seabed of the North Sea and form a threat to the safety at sea. A wide variety of warfare ammunition may be encountered and exposed with increasing human activities at sea (e.g. fisheries, dredging, harbour construction and wind-farm development). Mine detection is a priority in French, Belgian and Dutch waters. However, mines are usually not detected when they are completely covered with sediment, thus remaining a potential risk associated with all activities that disturb the seabed (NRC 2003).
Mine burial processes are commonly categorized into the following two groups: impact and post-impact burial (Wilkens and Richardson 2007). Burial by impact is well-known from literature (Mulhearn 1995, Chu et al. 2002, Abelev et al. 2007, Aubeny and Han 2007), and occurs when the mine (or object) falls freely through the water column. As the amount of burial is dependent on the bearing strength of the seabed sediment, burial by impact occurs mostly in areas with poorly consolidated muddy sediments. Post-impact mine burial is typically occurring in sandy bottoms and is mainly associated with sand-water-object interactions. As such, burial by scour is well-known in the fields of mine detection (e.g. Jenkins et al. 2007), maritime archaeology (e.g. Saunders 2005, Quinn, 2006) and marine engineering, such as seabed pipelines (e.g. Akoz et al. 2010). Scour occurs due to disturbance in the wave- or tide-induced flow caused by presence of obstacles such as pipelines. It typically manifests itself at the upstream face of the object (Saunders 2005, Garcia et al. 2009), and diminishes downstream of the obstacle, where scour-related depressions grade into depositional features (Inman and Jenkins 2005). The impact of waves on exposed mines accounts for most mine burial (e.g. Plager 2000, Voropayev et al. 2003, Hay and Speller 2005, Cataño-Lopera and Garcia 2006 a, Friedrichs and Trembanis 2006, Geurts et al. 2007, Grilli 2007, Traykovski et al. 2007, Trembanis et al. 2007, Wever and Luehder 2007). It forces the rollover of mines into scour pits, especially during storms. A second post-impact burial mechanism is related to migration of megaripples, causing periodical burial and exposure of object (Wever 2003, Cataño-Lopera and Garcia 2006 b, Cataño-Lopera et al. 2007, Wever and Luehder 2007, Garcia et al. 2009). This type of process occurs irrespective of the presence of the object, and also results from other changes in the (overall) seabed morphology, such as those resulting from seasonal changes in wave climate (Richardson and Briggs 2000, Jenkins et al. 2007). Additional burial mechanisms discussed in the literature are burial by fluidization associated with wave-induced failure in the sediment surrounding the mine (e.g. Brandes and Riggs 2002, 2004), and biological activity (Richardson and Briggs 2000).
The present study focuses on mine burial processes and on the predictability of mine burial in high-turbidity areas. A mine experiment was conducted in a mainly sandy seabed environment situated in Belgian coastal area (southern North Sea). The area is also characterised by the occurrence of high-concentrated mud suspensions (HCMS) (IMDC and WL 2007, Baeye et al. 2011). The latter are responsible for the short-term burial of the test mine, a mechanism that has to our knowledge never been described before. In the paper a detailed analysis is given of the daily patterns of mine burial and exposure by the formation and erosion of HCMSs superimposed on the longer-term burial controlled by storm waves. The paper also suggests that test mines can be used as an alternative instrumentation to study the dynamics of HCMS in high-turbidity areas.

6.2. *Environmental conditions*

The Belgian coastal zone is shallow (0-15 m below Mean Lower Low Water Spring (MLLWS)) with seabed sediments varying from pure sand to pure mud (Verfaillie et al. 2006). Highly turbid, coastal waters occur between Nieuwpoort and the Westerscheldt river mouth (Fig. 6.1). Suspended particulate matter (SPM) originates mainly from import from the Dover Strait and from erosion of Holocene mud layers in the coastal zone (Fettweis and Van den Eynde 2003). SPM concentrations may reach >3.0 g l^{-1} close to the bed. Mean tidal range at Zeebrugge is 4.3 m (2.8 m) at spring (neap) tide and maximum current velocities exceed 1.0 m s^{-1}. Tidal ellipses are commonly well-aligned with the coastline orientation. Typically, tides are responsible for more than 90% of the total variance observed in the time-series data of tidal elevation. The

associated amplitudes of the M2 and S2 dominant and semi-diurnal constituents are 1.8 and 0.5 m, respectively (Mouchet 1990). The rest of the total variance is explained by the occurrence of wind-induced flows. Significant sea set-up occurs with prevalent winds blowing from NW, and sea set-down occurs with SE winds. Wind forcing tends to bias the residual flow pattern (Yang 1998), and the SPM circulation along the Belgian coast (Fettweis et al. 2006, Fettweis et al. 2007, Baeye et al. 2011). Southwest winds are associated with recurring low-pressure weather systems (depressions) moving from the Atlantic Ocean towards Europe. High wind speeds may occur throughout the year; however, significant storms are abundant in the period October until March. Thus, significant wave heights are typically largest during fall and winter months in the southern North Sea. Salinity (range of 28-34 in the nearshore) varies with tides and wind forcing, and is fortnightly modulated (Lacroix et al. 2004). Winds blowing from the NE-E wind sectors coincide with decreasing salinity, as the influence of the Westerscheldt estuary increases. On the other hand, salinity increases under SW winds, when less turbid, open-Atlantic waters enter the study area through the English Channel.

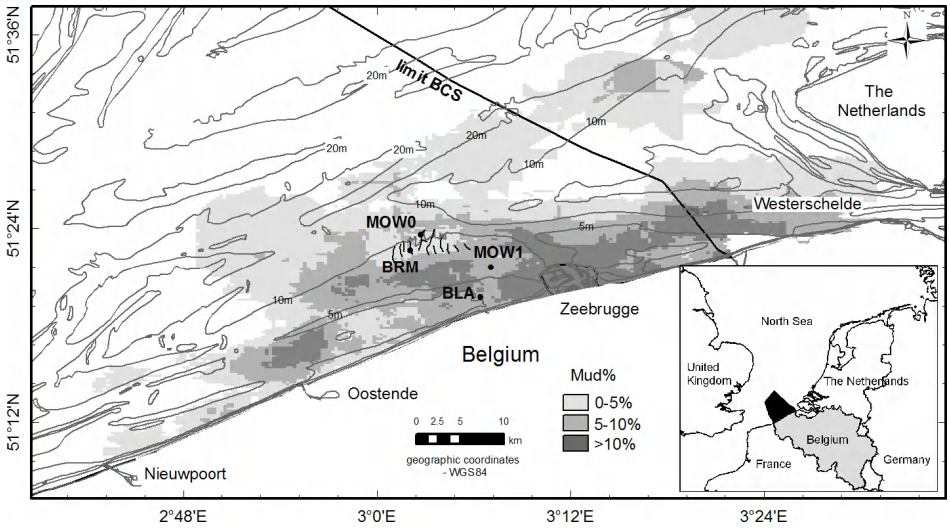

Figure 6.1 *Location of the mine experiment (BRM) in the southern Bight of the North Sea. The bathymetry (MLLWS) and mud content of the sandy seabed samples are given for the Belgian Coast. zone. Other monitoring stations in the area at the time of the experiment were MOW0 (Oceanographic station), MOW1 (benthic observatory) and BLA (investigated site in Baeye et al. 2011 - Chapter 2)*

6.3. *Methodology for data collection and analysis*

6.3.1. Mine burial experiment (BRM)

A mine burial experiment was conducted using test mines developed by the Forschungsanstalt der Bundeswehr für Wasserschall-und Geophysik (FWG, Fig. 6.2). The test mines have a diameter (D) of 0.47 m, are 1.7 m in length and weigh 509 kg (apparent weight in water 238 kg). Mine motion (pitch and roll) is recorded via a built-in, three-axis accelerometer. The mines were designed with three rings consisting of 24 optical sensor pairs (LED bridges). These are equally spaced around the mine at 15° intervals, both in the middle and at either end; this results in a range of vertical burial resolution or vertical bed evolution variations between 0.2 and 3 cm. The LED bridges rely on optical light transmission over a short path of 4 cm. "1" recordings

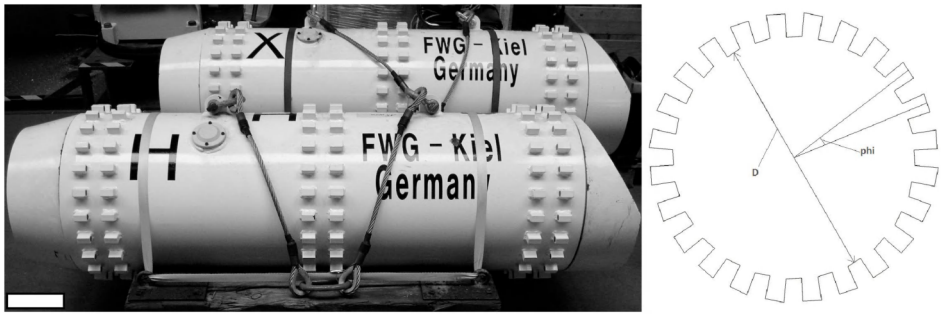

***Figure 6.2** (**left**) Pre-deployment photo of the test mines. The white bar in the lower left corner represents 20 cm. (**right**) BRM cross-section with D (47 cm), diameter, and phi, the angle between two successive LED housings. Mine burial diameter refers to the height of the mine (or mine ring) buried with respect to the lowest LED pair*

correspond to sediment hindering light propagation, whereas "0" recordings correspond to proper light propagation. The conceptual model of recording mines in sandy environments is based on the presence of bedforms (ripples, megaripples) that would cover the mine partially or completely, and temporally (dependent on the migration speed of the (mega-) ripples). On the other hand, hydrodynamics (tidal currents, storm waves) will also affect the burial stage of the mine, i.e. by scour. The signal per ring corresponds to the bed evolution measured vertically. When a sequence of burial and exposure is read in the signal from the three different rings, then typically one may state that ripples are passing the mine. The recording interval of 15 min in this experiment sets the limit of the time resolution. Variations occurring at periods less than 15 min are not fully characterized, and per 15 min interval, only the final result of pitch, roll and the number of buried sensor pairs is recorded (Wever and Luehder 2007). Mine burial is given either by the diameter B (per ring), or by the total mine burial volume (in %) taking into account all rings. The burial diameter is calculated as follow:

$$B = \frac{D}{2}\left(1 - \cos\left(\frac{n\varphi}{2}\frac{\pi}{180}\right)\right)$$

with n, the number of buried sensors ("1" recordings) and φ the angle interval of 15° (Fig. 6.2, right). Time-series data of mine burial were low-pass filtered to analyze longer-term (>33 hours) variability (see also 6.3.2). No "bad" recordings, caused by bio-fouling, were observed. The mines were deployed on a sandy seabed in water depths of 9 m -MLLWS. At the experiment's onset (September 25th, 2008 or year day 269), sonar imagery of the seabed revealed that both mines were oriented 115° True North (Fig. 6.3). The mine records lasted 104 days until January 6th, 2009.

6.3.2. *Meteorological, Oceanographic station and wave buoy (MOW0)*

During the mine experiment, current data were collected at MOW0, a measuring pole located about 1 km from the BRM site and in water depths of 10 m -MLLWS. An upward-looking Doppler current meter (Aanderaa®, DCM-12, 600 kHz) records burst data at 10-minute sampling intervals, with a ping rate of 4 Hz. The time-series was low-pass filtered to remove trends (i.e. tides) occurring at periods less than 33 hours (Beardsley et al. 1985). Each point was replaced with a weighted average of 33 hours on either side of the central point. Further, the two horizontal current components were rotated into a long- and cross-shore orthogonal coordinate system. The positive cross-shore axis is directed landward (T°155), and the positive longshore axis is northeastward (T°65). Wind speed and directions (meteorological convention) were recorded at 25 m above MLLWS at MOW0, and converted following the oceanographic convention. Wind shear stresses were estimated using the adjusted wind data for 10 m above MLLWS (U_{10}) and by introducing a neutral drag coefficient (C_{DN}) (Large and Pond 1981):

$$C_{DN} = 1.2\ 10^{-3}, \text{ for } 4 \text{ m s}^{-1} \leq U_{10} \leq 11 \text{ m s}^{-1},$$

$$C_{DN} = \left(0.49 + 0.065\, U_{10}\right) 10^{-3}, \text{ for } 11 \text{ m s}^{-1} < U_{10} \leq 25 \text{ m s}^{-1}.$$

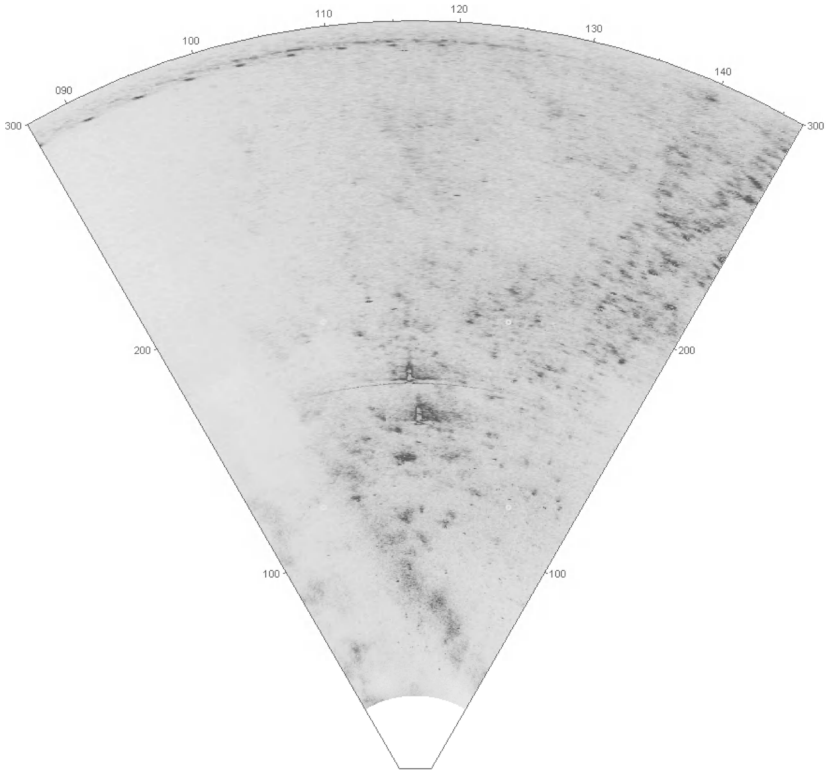

Figure 6.3 *Image of the test mines on the seabed, as obtained by MCMV (mine counter measure vessel) hull-mounted sonar. Both mines are oriented 115° true north (toward the top of the page), and they are situated about 150-200 meters from the sonar*

6.3.3. Benthic observatory

During part of the mine experiment, a benthic tripod was deployed at a more inshore location (MOW1, see Fig. 6.1) with same water depth (9 m –MLLWS) for a time period of 25 days (days 322 – 347). A SonTek® 3 MHz Acoustic Doppler Profiler (ADP) (2.25 mab), a SonTek® 5 MHz Acoustic Doppler Velocimeter (ADV) (0.35 mab) and two D&A® Optical Backscatter Sensors (OBS) (2.25 & 0.25 mab) recorded on the tripod (http://www.mumm.ac.be/EN/Monitoring/Belgica/tripod.php). All time-series data were stored in two SonTek® Hydra data logging systems. Calibration of the OBS's was carried out for several tidal cycles in the nearshore area; a linear regression between OBS-NTU and SPM concentrations from water sample treatment was obtained (cf. Fettweis 2008). In addition to the currents, the ADV also measured continuously the distance between the sensor and the top of the 5 MHz acoustic detection layer. However, when HCMSs near the bed (eventually fluid mud) reach the ADV measuring volume, both the current measurements and boundary layer detection may become erroneous. Defining the acoustic boundary layer is known to perform well for a sandy seabed (Velasco and Huhta 2010); however, recently it was also used successfully in delineating the upper boundary of a poorly defined mud beds (Baeye et al. 2011).

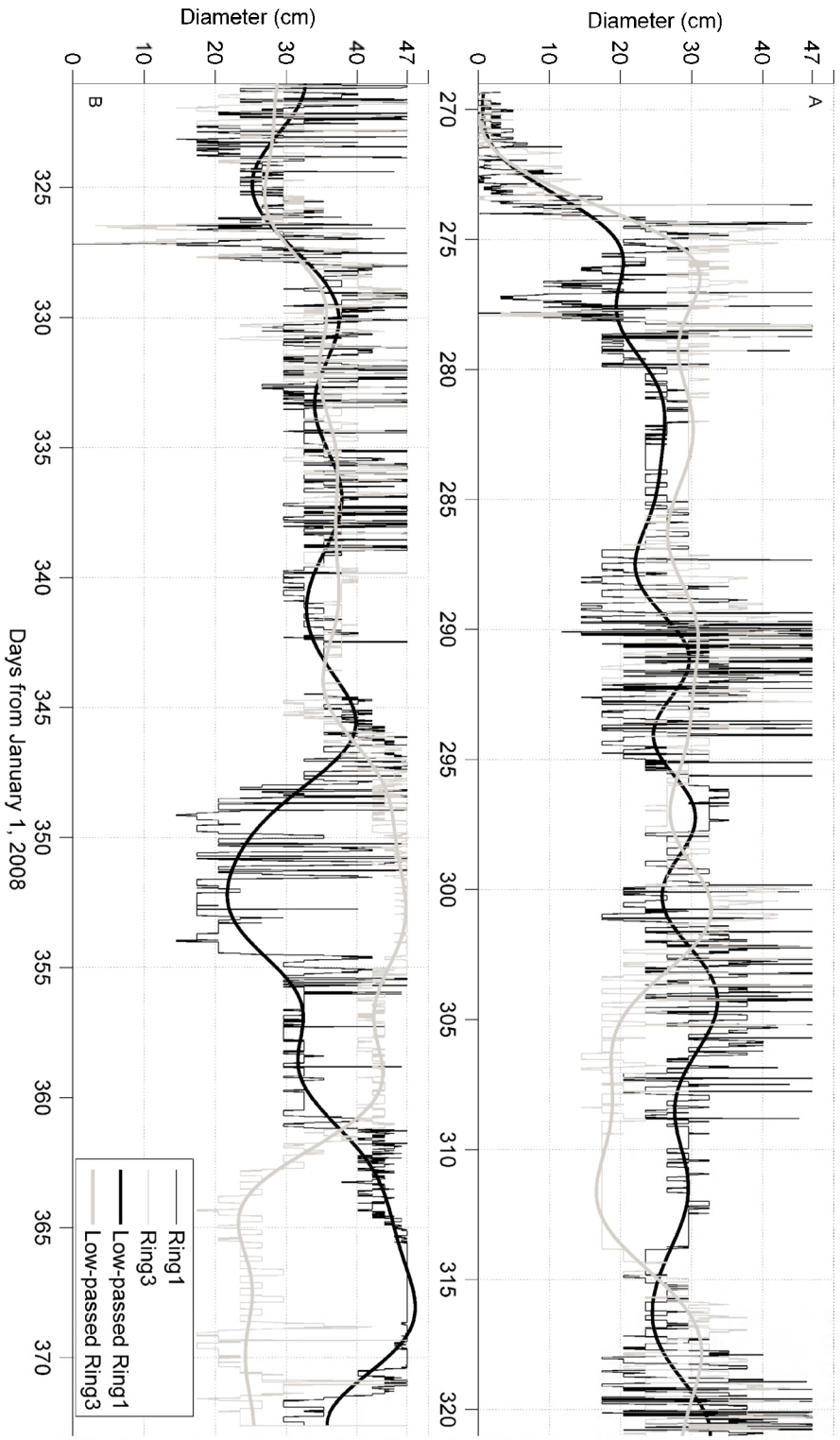

Figure 6.4 *Time-series data of mine rings 1 and 3, together with their low-passed filtered curves for days 269-321 (**a**), and for days 321-373 (**b**)*

It is difficult to detect this type of boundary because it is a strong concentration gradient (lutocline) rather than a sharp water-sediment interface. To overcome the issue of failing ADV boundary detections, Baeye et al. (2011) used a technique based on the ADP backscatter intensity. It considers the first high return in the backscattered signal (i.e. beam has hit the boundary), then it selects 5 bin values on either side of the maximum value, and fits a quadratic equation to them. The location of the maximum value found, represents the top of the 3 MHz acoustic detection layer. Further, a classification of 40 tidal cycles was realized for a mean tidal range of 3.6 m and distinguishing neap tides and spring tides.

6.3.4. *Acoustic surveys*

Repeated surveys were conducted to monitor the changing seabed morphology, and to visualize the mine burial stage and heading of the mines. Different instruments were used: an automated underwater vehicle (AUV-REMUS100 with 900 kHz frequency sonar), a pole-mounted multi-beam system (EM1002s, 100 kHz) and towed side-scan sonar (KLEIN 3000 series, 100 and 500 kHz).

6.3.5. *Hydrodynamic numerical model*

The currents, surface elevation and turbulent kinetic energy were modelled using an implementation of the COHERENS V2.0 hydrodynamic model to the Belgian Continental Shelf. This 3D model (OPTOS-BCZ) solves the continuity and momentum equations on a staggered sigma coordinate grid with an explicit mode-splitting treatment of the barotropic and baroclinic modes. A description of the COHERENS model can be found in Luyten et al (1999) and Luyten (2011). OPTOS-BCZ covers an area between 51°N and 51.92°N and between 2.08°E and 4.2°E. The horizontal resolution is 0.71' (longitude) and 0.41' (latitude), corresponding to a grid size of about 800 m. Boundary conditions of water elevation and depth-averaged currents for this model were provided by the operational models OPTOS-NOS (covering the North Sea) and OPTOS-CSM (covering the North-West European Continental Shelf) of the Management Unit of North Sea Mathematical Models (see www.mumm.ac.be). Pison and Ozer (2003) and Dujardin et al (2010) validated the current velocities of OPTOS-BCZ using ADCP measurements. The bottom shear stress for currents alone was determined using the calculated current velocity in the lowest layer of the model and using a bottom roughness length of 0.35 cm. The latter is based on the most significant seabed ripples or dunes (i.e. interact most with the flow). Therefore, the roughness length is given by the ratio between the square of the dunes height and their wavelength. The aim of using the model is estimating the hydrodynamics at the mine site, since no in-situ recordings of currents were realized.

6.4. *Results*

6.4.1. *Mine burial*

The time-series data derived from mine rings 1 and 3 (outer end rings) recordings show high variability over time (Fig. 6.4). Their low-passed signals show an opposite burial behaviour indicating opposing trends of increased burial and exposure occurring at the mine ends. The shorter-term (intra-tidal) variations are more easily observed in Fig. 6.5, which shows only four tidal cycles with corresponding near-bed current components. At maximum ebb and flood (see highlights in Fig. 6.5), one signal corresponds to more exposure and the other with increase in burial. This pattern occurs for almost 75% of the time, corresponds with relative bed-level changes of 10-15 cm around the mine.

6.4.2. *Meteorological influence*

SSW-SW winds were the strongest and most abundant during the experiment, followed by winds blowing from the NW sector. NE and E winds were weaker and less common. The wind changed direction frequently, with drops in pressure and low sea

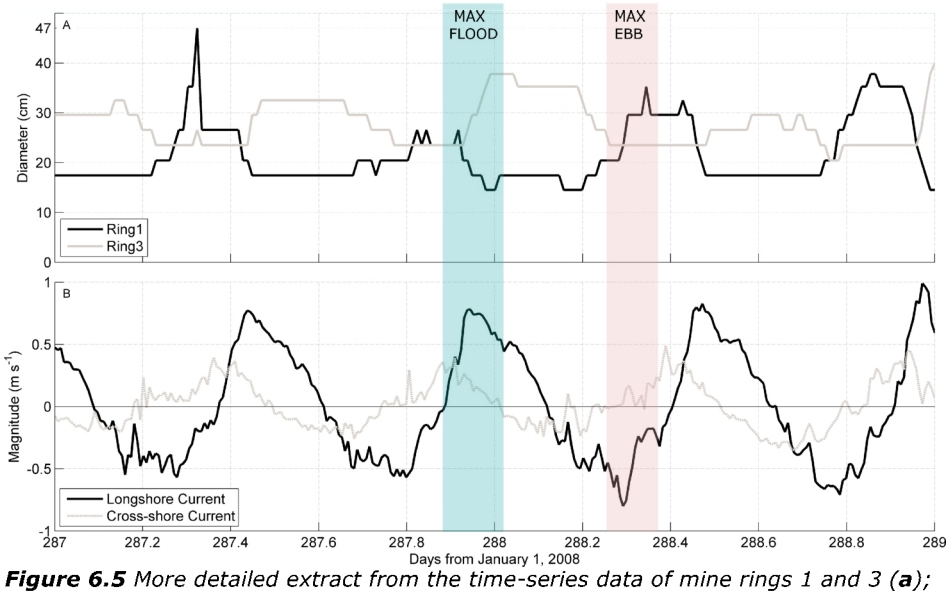

Figure 6.5 *More detailed extract from the time-series data of mine rings 1 and 3 (**a**); and the corresponding longshore and cross-shore currents (**b**) for a period of 2 days (~4 tidal cycles). The currents were recorded at 3 meters above bed*

surface levels corresponding to periods with southerly winds. Meteorological observations show evidence of two storms that forced sizable short-term increases in sea level and significant wave height (figs. 6.6, 6.7). During these storms, which represent only 1% of the monitoring time, the significant wave height (averaging 0.8 m with a mean period of 4 s) increased to more than 2.5 m.
Significant mine burial is associated with the passage of these storms. A first storm impacted the area in October 2008 (days 275-277), generating significant wave heights of more than 2.5 m (Fig. 6.8). Minor mine roll was recorded, together with increased mine burial. In addition, a reorientation was likely to be induced by the storm action (as observed in sonar images between both storms). A second storm event, with wave heights of up to 3.5 m, hit the area in November 2008 (days 326-328). As a result, the mine rolled 90°. During both storms, short-term formation of scour pits and the associated exposure of the outer ends of the mines were followed by the mines rolling into the pits. They settle at a greater depth relative to the seabed. Increased burial followed when the wave energy returned to fair-weather values and the scour pit quickly filled up with sediments.
When comparing low-passed mine behaviour to wind-stress measurements, it is clear that wind direction is one of the parameters governing longer-term mine burial (Fig. 6.9). During periods of E-NE winds (wind stress toward the W-SW) ring 1 was buried deeper than ring 3. During periods of prevailing SW winds, the opposite was true. Therefore, meteorological conditions may explain the contribution of wind forcing to mine burial behaviour on the longer term.

6.4.3. Suspended particulate matter (SPM)

The acoustic layer detection derived from the acoustics on the benthic tripod show good agreement with the mine burial data (Fig. 6.10). The ADV signal is hard to read, since its time-series is discontinuous, explained by either attenuation of the acoustic signal and/or an increase in HCMS thickness reaching and disturbing the ADV sampling volume. Although the match is far from perfect, the three signals show synchronous periodic rises and falls of the top of the boundary layer. The rises correspond with SPM settling out of the water column during ebb slack tide (i.e. slack water after high water, red highlights in Fig. 6.10) and flood slack tide (i.e. slack water after low water, blue highlights in Fig. 6.10). This is observed under both spring and neap tide phases (Figs. 6.11 and 6.12).

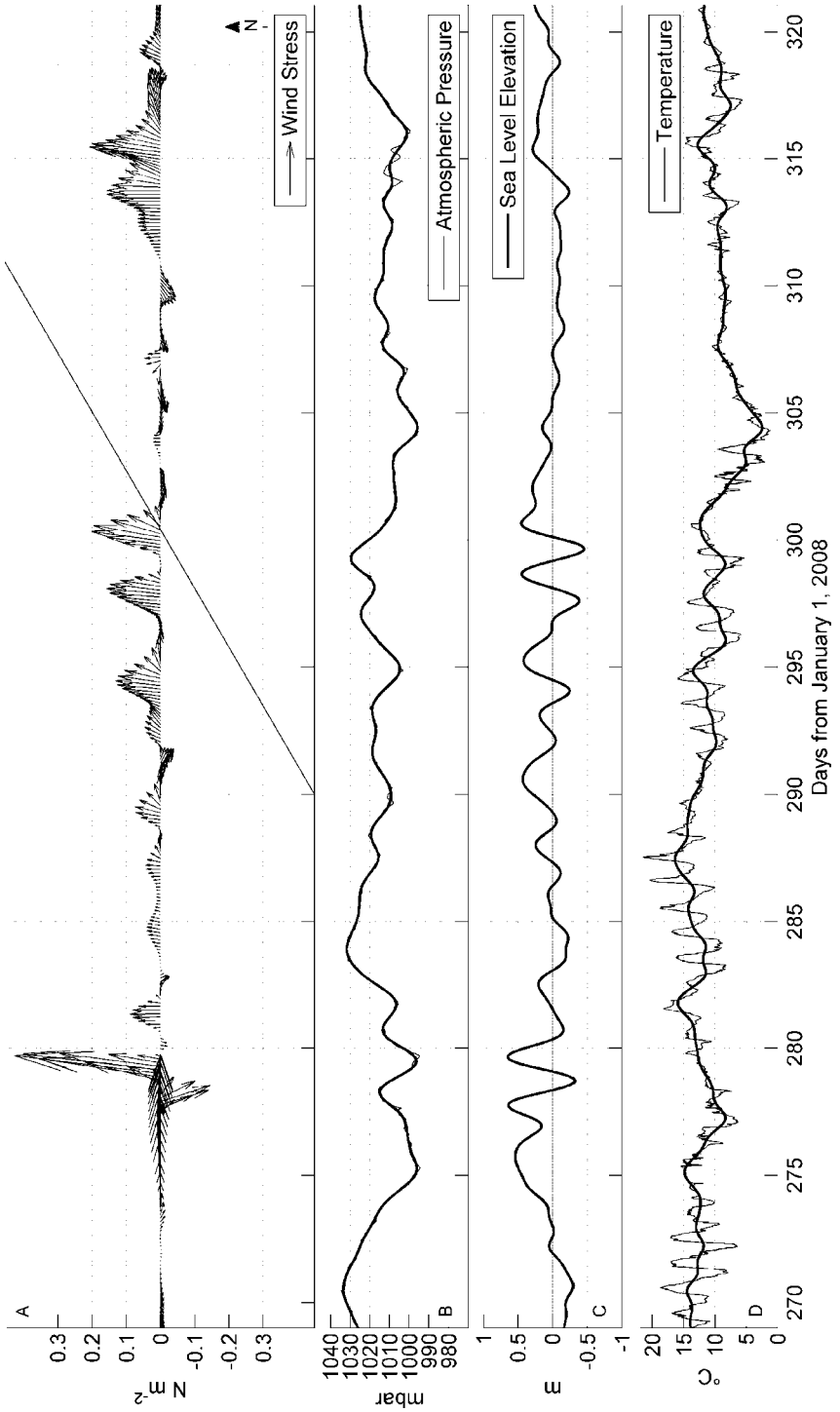

Figure 6.6 *Meteorological records for days 269-321: (**a**) wind stress; (**b**) atmospheric pressure; (**c**) sea level and (**d**) temperature. In the wind stress time-series, north is indicated with arrow*

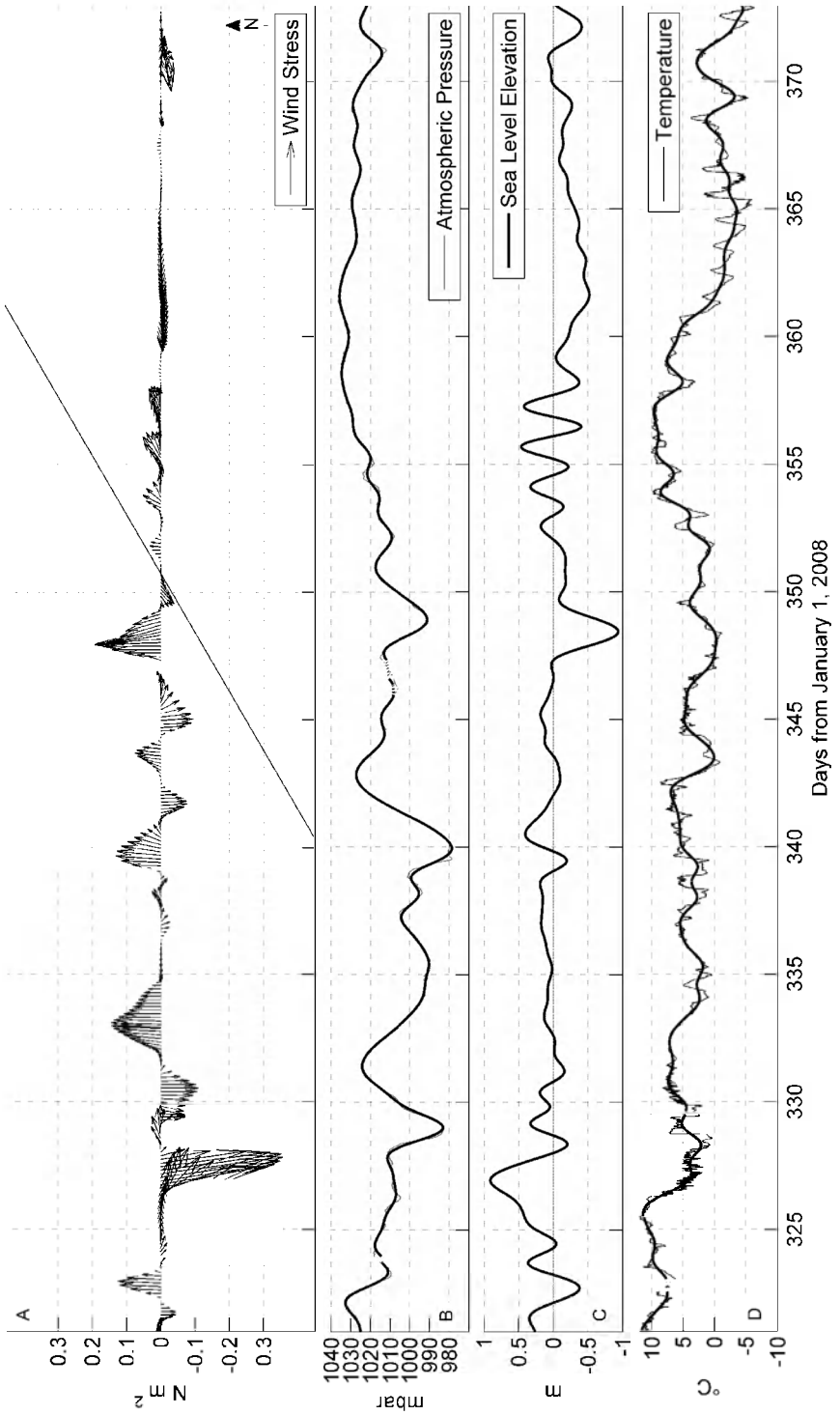

Figure 6.7 *Meteorological records for days 269-321: (**a**) wind stress; (**b**) atmospheric pressure; (**c**) sea level and (**d**) temperature. In the wind stress time-series, north is indicated with arrow*

Generally, SPM concentration (2 mab) is in line with the tidal forcing, with re-suspension peaks at maximum ebb and maximum flood, and SPM settling during slack tide. The observed rises of the boundary layer reach up to 25 cm around ebb slack tide and up to 7 cm at flood slack tide. SPM concentrations at 2 mab are significantly different from those at 0.2 mab; the latter also reflecting the boundary layer rises and falls.

6.4.4. Seabed characteristics

The mine experiment was conducted 9 km off the coast where large, N-S oriented sand dunes define the overall underwater landscape. These bed forms are several meters in height and hundreds of meters in length (see black lines for mapped sand waves in Fig. 6.1 near "BRM"). Smaller dunes (megaripples) with a maximum height of 0.5 m and wave length of a few meters are superimposed on these dunes. No-well defined bed forms were visible on the acoustic data collected during the mine experiment. However, a survey conducted after the mine stopped recording when its battery died (January 2009) showed megaripples of up to 30 cm in height and up to 7 m in wave length. Seabed samples collected with a box-corer in the proximity of the mine and by divers directly around the mine. Sand (with intercalations of mud) and compacted mud (Holocene) was sampled, often covered with fresh mud. Rather coarse sands (550 µm), compared with the medium-grained sand (450 µm) away from the mine, were found in the divers' samples at the mine site. Also, a secondary silt-grain size modus was found in the samples.

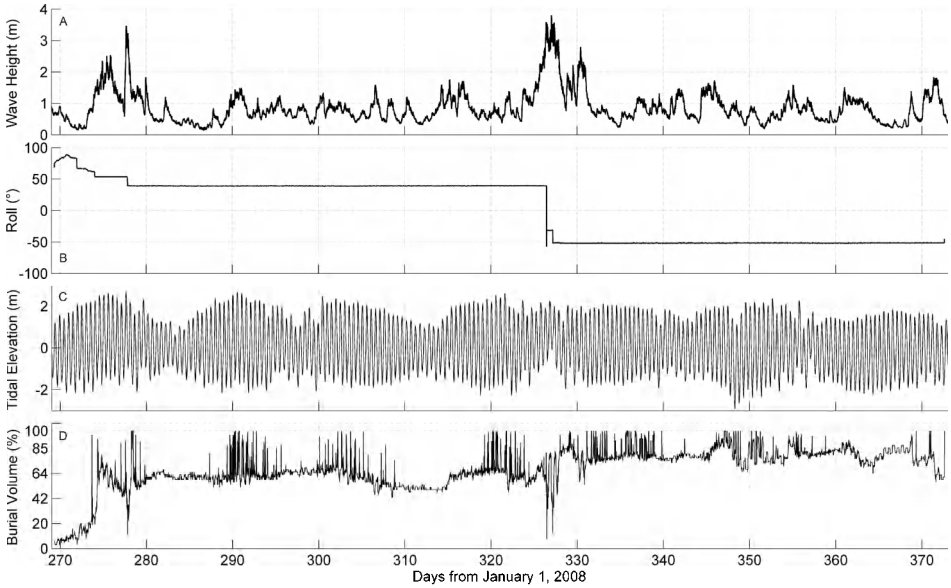

Figure 6.8 *Meteorological records for days 269-321: (**a**) wind stress; (**b**) atmospheric pressure; (**c**) sea level and (**d**) temperature. In the wind stress time-series, north is indicated with arrow*

6.5. Discussion

In literature, mine burial is linked to several processes (cf. Wilkens and Richardson 2007). On a sandy seabed, the most important one is burial by scour as a result of sand-water-object interactions. Our data show that SPM dynamics is also a possible mine burial driver. This process, which has not been linked to mine burial before, may be very important in high-turbidity environments with thick HCMSs. Table 6.1 summarizes all three types of burial processes (i.e. by HCMS, by scour, by storm waves) regarding their occurrences and maximum burial potentials during the monitoring period.

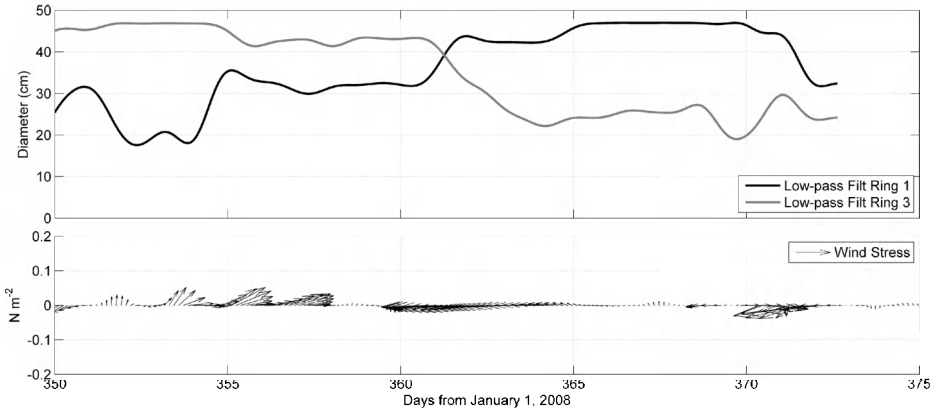

Figure 6.9 *Extract from the mine burial time-series (days 350-372).* ***Below****, wind stress; and* ***above****, two burial rings (at mine ends)*

Table 6.1 *Mine burial behaviour (occurrences and burial volumes) for the three types of mine burial*

	occurrence (time)	max burial (cm)
by scour	75%	15
by HCMS	10%	15
by storm	2%	30

6.5.1. Mine burial by scour-and-deposition cycles

Wave-induced scour and subsequent deposition in scour pits are responsible for most of the mine burial, especially on sandy seabeds. The signal of the mine burial volume is dominated by 2 main stages that are related to high-energy wave events: (1) 60% burial was reached after the first storm, which impacted the area a few days after the mine was placed on the seabed; (2) 80% mine burial was reached after a second, more severe storm. In this respect, (Cataño-Lopera and Garcia 2006 a) remarked the importance of the angle of attack. In our case, the initial angle of 115°T (Fig. 6.3) changed during the first storm to 65°T as revealed from the acoustic imagery of the seabed. This alignment was in correspondence with the storm waves propagating towards the S-SE under the N-NW wind conditions. This new orientation was practically parallel to the principal axis of the tidal current ellipse; as such no further alignments of the mines were observed afterwards. This leads to symmetrical conditions of the flow and sediments around the mine, similar to the observations of (Cataño-Lopera and Garcia 2006 a, Cataño-Lopera et al. 2007). It is known that tidal forcing affect the mine ends with scour and deposition cycles on a quarter-diurnal basis (Brandes 1999, Brandes and Riggs 2004). Our data show that for most of the time no substantial changes in the total mine burial volume occurred. However, variations in the burial volume were observed when a wind-driven flow was sustained. As a result, enhanced scouring on one mine end occurred over several days (Fig. 6.9). As similar with tidal forcing, flow vortices in the upstream end of the mine object increase scouring (Richardson and Briggs 2000, Saunders 2005, Friedrichs and Trembanis 2006). Because of bedload transport and seabed erosion, winnowing of finer sand (and silt/clay) fractions is likely to occur (Friedrichs and Trembanis 2006). This might explain the rather coarse sands (550 μm) in the divers' samples at the mine site, collected prior to mine recovery.
Based on seabed images (e.g. Fig. 6.3), no megaripples were observed in the very direct proximity of the mine during the experiment. However, the area might show the presence of this type of bedforms; as such, this burial mechanism cannot be just ruled out. Nonetheless, megaripple migration cannot account for short-term burial pattern because it is a process unrelated to semi-diurnal slack-time periodicity.

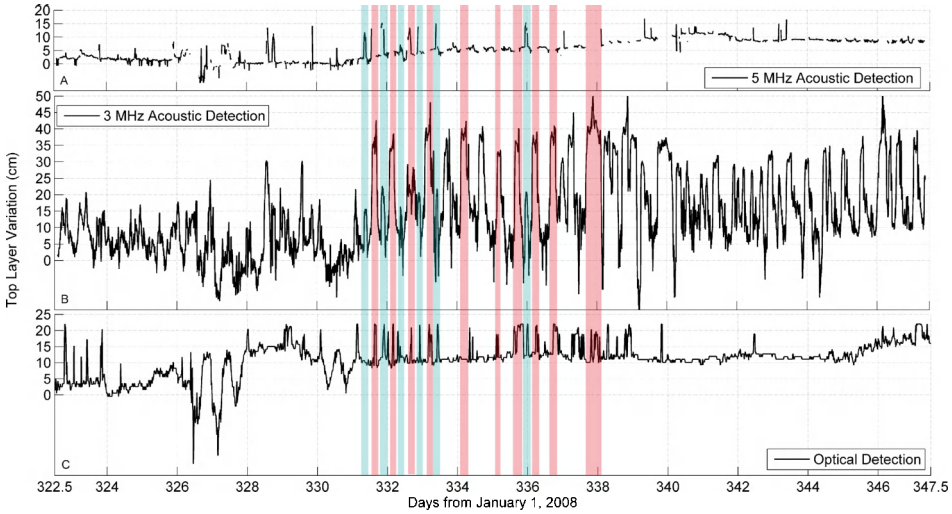

Figure 6.10 *Time-series of vertical seabed changes by means of ADV (**a**), ADP (**b**) and BRM (**c**). a, b are recordings at MOW1, and c at BRM (nearby MOW0). Optical and acoustic instruments detect HCMS layer formation. ADV shows many gaps, and the ADP shows high rises up to 25 cm. Near-synchronicity of the main peaks strongly suggests that HCMS formation and disintegration played a role in the burial and exposure of the test mine. Blue and red highlights show flood and ebb slack tides, respectively*

6.5.2. Mine burial by transient HCMSs

Wave-induced scour and subsequent deposition in scour pits are responsible for most of the mine burial, especially on sandy seabeds. The signal of the mine burial volume is dominated by 2 main stages that are related to high-energy wave events: (1) 60% burial was reached after the first storm, which impacted the area a few days after the mine was placed on the seabed; (2) 80% mine burial was reached after a second, more severe storm. In this respect, (Cataño-Lopera and Garcia 2006 a) remarked the importance of the angle of attack. In our case, the initial angle of 115°T (Fig. 6.3) changed during the first storm to 65°T as revealed from the acoustic imagery of the seabed. This alignment was in correspondence with the storm waves propagating towards the S-SE under the N-NW wind conditions. This new orientation was practically parallel to the principal axis of the tidal current ellipse; as such no further alignments of the mines were observed afterwards. This leads to symmetrical conditions of the flow and sediments around the mine, similar to the observations of (Cataño-Lopera and Garcia 2006 a, Cataño-Lopera et al. 2007). It is known that tidal forcing affect the mine ends with scour and deposition cycles on a quarter-diurnal basis (Brandes 1999, Brandes and Riggs 2004). Our data show that for most of the time no substantial changes in the total mine burial volume occurred. However, variations in the burial volume were observed when a wind-driven flow was sustained.
As a result, enhanced scouring on one mine end occurred over several days (Fig. 6.9). As similar with tidal forcing, flow vortices in the upstream end of the mine object increase scouring (Richardson and Briggs 2000, Saunders 2005, Friedrichs and Trembanis 2006). Because of bedload transport and seabed erosion, winnowing of finer sand (and silt/clay) fractions is likely to occur (Friedrichs and Trembanis 2006). This might explain the rather coarse sands (550 μm) in the divers' samples at the mine site, collected prior to mine recovery.
Based on seabed images (e.g. Fig. 6.3), no megaripples were observed in the very direct proximity of the mine during the experiment. However, the area might show the presence of this type of bedforms; as such, this burial mechanism cannot be just ruled out. Nonetheless, megaripple migration cannot account for short-term burial pattern because it is a process unrelated to semi-diurnal slack-time periodicity.

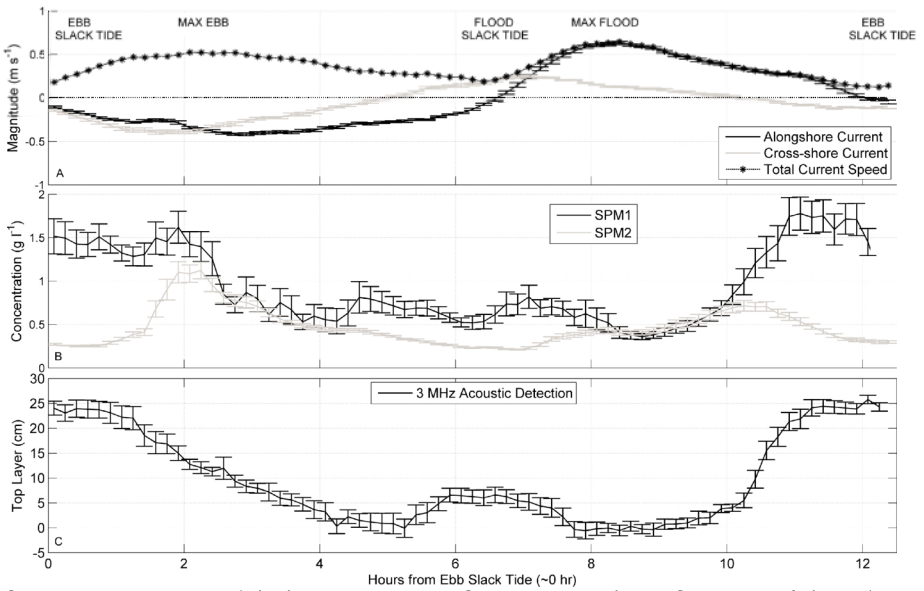

Figure 6.11 *Spring tidal-phase averages of time-series data of currents (**a**), sediment suspension (**b**), and HCMS dynamics (**c**). SPM1 and SPM2 are for 0.2 and 2 mab, respectively*

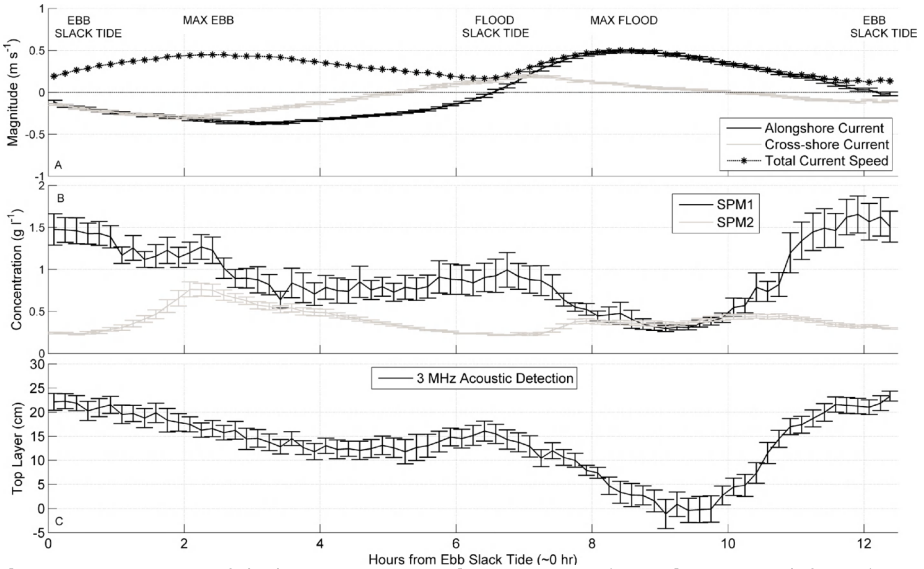

Figure 6.12 *Neap tidal-phase averages of time-series data of currents (**a**), sediment suspension (**b**), and HCMS dynamics (**c**). SPM1 and SPM2 are 0.2 and 2 mab, respectively*

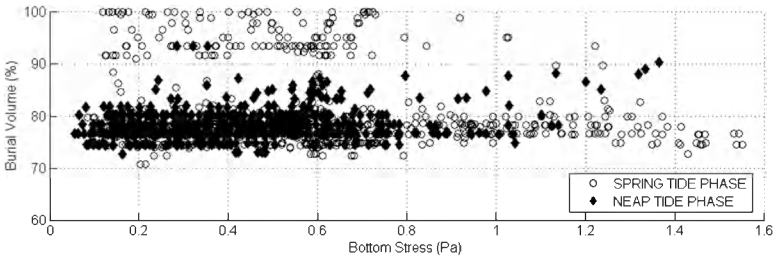

Figure 6.13 *Hydrodynamic model results (mine site) of bottom stress plotted against the mine burial volume indicate that phases with 90-100 % of mine burial coincide with slack tides (bottom stresses <0.7 Pa) during spring tide phases. Neap tide phases do not show any increased burial*

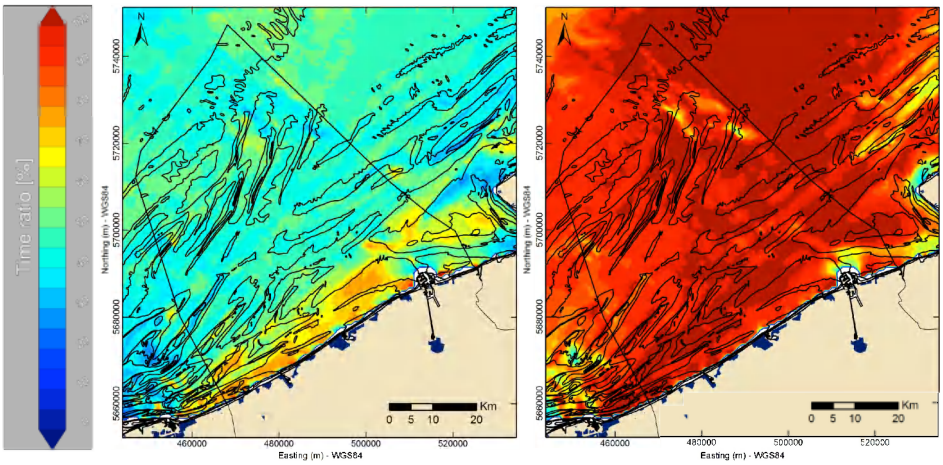

Figure 6.14 *Model results of slack tide ratio over two tidal cycles (neap tide,* ***right*** *and spring tide,* ***left****). Slack tide is here defined as when bottom shear stresses are less than 0.7 Pa; this is in accordance with erosion resistance measurements of bed samples taken in the study area (Fettweis et al. 2010). Blue is 0% and red 100% time ratio. Figure illustrates the high temporal variability (contrast between neap and spring) in hydrodynamics and in the potential of mine burial by HCMS as such*

6.6. Conclusions

Time-series data recorded by a test mine has been analyzed in combination with hydrodynamic and meteorological recordings, and a shorter time-series data of suspended sediment concentration. Nearby the port of Zeebrugge, the study area is characterized by highly turbid waters. However, the sandy seabed seems to be responsible for a well-known burial process that is related to scour by storm waves. This process accounts for most of the mine burial volume (60 and 80%). Tidal forcing will also account for some scour of the seabed around the mine. Furthermore, the hydrodynamic pattern present in the study area can be biased by changing wind conditions. As a result, subtidal flow forcing is acting on the mine as well.
Superimposed on the mine burial by scour signal, a more cyclic (quarter-diurnal) burial signal occurred preferably during spring tide phases. Benthic observations of SPM concentration and changing seabed evolution have shown that during slack tides, the mine is covered with HCMS layer. An acoustic (3 MHz) detection method reveals these bed boundary level changes (up to 25 cm), in accordance to what is observed by the optics-based test mine measurements. The potential of the test mine detecting HCMS layers has been proven by the authors, and mine burial by transient HCMS is introduced. The latter has implications towards mine hunting strategies. In order to assess the possibility that mines in HCMS areas are missed during tracking surveys,

additional experiments will have to be conducted in areas with mud suspensions of various thickness and stability. Areas and circumstances where HCMSs are relatively persistent should be monitored and analyzed in detail as part of follow-up studies. For Belgium, the areas with highest risk are closest to shore during neap tides, when burial is potentially the most prolonged.

6.7. *Acknowledgments*

The presented results were obtained thanks to the cooperation between the Bundesamt für Wehrtechnik und Beschaffung - Forschungsanstalt der Bundeswehr für Wasserschall-und Geophysik (BWB - FWG, Germany), the Belgian Naval Defence - Direction Générale Material Resources (DGMR) and the Management Unit of the North Sea Mathematical Models (MUMM). The first author (M. Baeye) acknowledges a specialization grant from IWT (Agency for Innovation by Science and Technology, Flanders). Research at MUMM was partly funded by the Maritime Access Division of the Ministry of the Flemish Community (MOMO project) and by Belgian Science Policy (Science for a Sustainable Development, QUEST4D project, SD/NS/06A). T. Wever and R. Lühder (FWG) are thanked for their assistance on the preparation and deployment of the FWG burial recording mines. L. Vigin (MUMM) is thanked for her assistance on creating the GIS figure 6.14. The captains and their crews of Belgian Navy's minehunters Lobelia and Primula are acknowledged for the skilful deployment and recuperation of the test mines. G. Dumon (Ministery of the Flemish Community, Maritime Services, Coast. Division/Hydrography) made available wind and wave measurement data. We also want to acknowledge the crew of RV Belgica for mooring and recuperation of the tripod; and, A. Pollentier and L. Naudts and their team (Measuring Service of MUMM, Oostende) for technical support. The two reviewers are thanked for their constructive remarks.

6.8. *References*

Abelev, A.V., Valent, P.J., Holland, K.T., 2007. Behavior of a Large Cylinder in Free-Fall through Water. Oceanic Engineering, IEEE Journal 32, 10-20.

Akoz, M.S., Sahin, B., Akilli, H., 2010. Flow characteristic of the horizontal cylinder placed on the plane boundary. Flow Measurement and Instruments 21, 476-487.

Aubeny, C.P., Han, S., 2007. Effect of Rate-Dependent Soil Strength on Cylinders Penetrating Into Soft Clay. Oceanic Engineering, IEEE Journal of 32, 49-56.

Baeye, M., Fettweis, M., Voulgaris, G., Van Lancker, V., 2011. Sediment mobility in response to tidal and wind-driven flows along the Belgian inner shelf, southern North Sea. Ocean Dynamics, 1-12.

Beardsley, R.C., Limeburner, R., Rosenfeld, L.K., 1985. Introduction to the CODE-2 moored array and large-scale data report, in: Limeburner, R. (Ed.), CODE-2: Moored array and large-scale data report. WHOI, Massachusetts, p. 234.

Brandes, H.G., 1999. Mine Burial due to Wave-induced Liquefaction and Other Processes, 9th Int. Offshore and Polar Eng. Conf., Brest, France, p. 568:574.

Brandes, H.G., Riggs, H.R., 2002. Modeling of Seabed Liquefaction and Other Processes Responsible for Mine Burial. ASME Conf. Proc. 2002, 455-462.

Brandes, H.G., Riggs, H.R., 2004. Modeling of Sediment Mechanics for Mine Burial Prediction. University of Honolulu, p. 11.

Cataño-Lopera, Garcia, M.H., 2006 a. Burial of Short Cylinders Induced by Scour under Combined Waves and Currents. Journal of Waterway, Port, Coastal, and Ocean Engineering 132, 11.

Cataño-Lopera, Y.A., Demir, S.T., Garcia, M.H., 2007. Self-Burial of Short Cylinders Under Oscillatory Flows and Combined Waves Plus Currents. Oceanic Engineering, IEEE Journal 32, 191-203.

Cataño-Lopera, Y.A., García, M.H., 2006 b. Geometry and migration characteristics of bedforms under waves and currents. Part 1: Sandwave morphodynamics. Coastal Engineering 53, 767-780.

Chu, P.C., Smith, T.B., Haeger, S.D., 2002. Mine Impact Burial Prediction Experiment, J. of Counter-Ordnance Technology, p. 10.

Dujardin, A., Van den Eynde, D., Vanlede, J., Ozer, J., Delgado, R., Mostaert, F., 2010. BOREAS – Belgian Ocean Energy Assessment: A comparison of numerical tidal models of the Belgian part of the North Sea. Version 2_0. WL Rapporten, 814_03. Flanders Hydraulics Res., Soresma & MUMM: Antwerp, Belgium. BELSPO contract SD/NS/13A

Fettweis, M., 2008. Uncertainty of excess density and settling velocity of mud flocs derived from in-situ measurements. Estuarine, Coastal and Shelf Sciences 78, 426-436.

Fettweis, M., Francken, F., Pison, V., Van den Eynde, D., 2006. Suspended particulate matter dynamics and aggregate sizes in a high turbidity area. Marine Geology 235, 63-74.

Fettweis, M., Francken, F., Van den Eynde, D., Verwaest, T., Janssens, J., Van Lancker, V., 2010. Storm influence on SPM concentrations in a coastal turbidity maximum area with high anthropogenic impact (southern North Sea). Continnetal Shelf Research 30, 1417-1427.

Fettweis, M., Nechad, B., Van den Eynde, D., 2007. An estimate of the suspended particulate matter (SPM) transport in the southern North Sea using SeaWiFS images, in-situ measurements and numerical model results. Continental Shelf Research 27, 1568-1583.

Fettweis, M., Van den Eynde, D., 2003. The mud deposits and the high turbidity in the Belgian-Dutch coastal zone, southern bight of the North Sea. Continental Shelf Research 23, 669-691.

Friedrichs, C.T., Trembanis, A.C., 2006. Forecasting Scour Related Mine Burial Using a Parameterized Model. School of Mar. Sci., Virginia Institute of Mar. Sci., Gloucester Point, VA, p. 12.

Garcia, M.H., Cataño-Lopera, Y.A., Landry, B.J., 2009. Mine Burial by Local Scour and Sand Waves. Illinois, Urbana Dept of Civil and Environmental Engineering, pp. 11.

Geurts, B.J., Clercx, H., Uijttewaal, W., Voropayev, S., Testik, F., Fernando, H., Balasubramanian, S., 2007. Sediment transport, ripple dynamics and object burial under shoaling waves, Particle-Laden Flow, pp. 15-27.

Grilli, S.T., 2007. Wave Induced Mine Burial and Sediment Transport in Coastal Environment: Wave and Sediment Transport Modeling Studies. Dept of Oceanic Engineering, Kingston, Rhode Island, p. 12.

Hay, A.E., Speller, R., 2005. Naturally occurring scour pits in nearshore sands. Journal Geophysical Research 110, 15.

Inman, D.L., Jenkins, S.A., 2005. Scour and Burial of Objects in Shallow Water, in: Schwartz, M.L., Kearney, M., Stevenson, J. (Eds.), North America, Coast. Ecology. Encycl. Coastal Sciences pp. 714-721.

IMDC; WL (2007). Langdurige monitoring van zout/zoet-verdeling in de haven van Zeebrugge en monitoring zoutconcentratie slibconcentratie en hooggeconcentreerde slibsuspensies in de Belgische kustzone. Waterbouwkundig Laboratorium: Borgerhout. International Marine and Dredging Consultants Rep.

Jenkins, S.A., Inman, D.L., Richardson, M.D., Wever, T.F., Wasyl, J., 2007. Scour and Burial Mechanics of Objects in the Nearshore. Oceanic Engineering, IEEE Journal 32, 78-90.

Lacroix, G., Ruddick, K., Ozer, J., Lancelot, C., 2004. Modelling the impact of the Scheldt and Rhine/Meuse plumes on the salinity distribution in Belgian waters (southern North Sea). Journal of Sea Research 52, 149-163.

Large, W.G., Pond, S., 1981. Open Ocean Momentum Flux Measurements in Moderate to Strong Winds. Journal of Physical Oceanography 11, 13.

Luyten, P. J., Jones, J. E., Proctor, R., Tabor, A., Tett, P., Wild-Allen, K. 1999. COHERENS, a coupled hydrodynamical-ecological model for regional and shelf seas: User Documentation. MUMM report, Brussels, Belgium. 911 pp. http://www.mumm.ac.be/coherens.

Luyten P.J., 2011. COHERENS — A Coupled Hydrodynamical-Ecological Model for Regional and Shelf Seas: User Documentation. Version 2.0. RBINS-MUMM Report, Royal Belgian Institute of Natural Sciences.

Mouchet, 1990. Analysis of tidal elevation and currents along the Belgian Coast, Tech. Rep. G.H.E.R. University of Liège Sart Tilman, Liège.

Mulhearn, P.J., 1995. Experiments on Mine Burial or Impact - Sydney Harbour, Technical Note. Aeronautical and Maritime Res. Laboratory, Melbourne, p. 18.
NRC, 2003. Environmental Information For Naval Warfare. National Academies Press.
Pison, V., Ozer, J. 2003. Operational products and services for the Belgian coastal waters. In: Building the European capacity in operational modeling, Proc. 3rd Int. Conf. on EuroGOOS (Dahlin, H., Flemming, N.C., Nittis, K., Petersson, S.E., eds.). Oceanic Seriers 69, 503-509.
PIANC, 2008. Minimizing harbour siltation, p. 75.
Plager, W.L., 2000. Mine Burial in the Surf Zone, Naval Postgraduate School Monterey, CA, p. 66.
Quinn, R., 2006. The role of scour in shipwreck site formation processes and the preservation of wreck-associated scour signatures in the sedimentary record evidence from seabed and sub-surface data. Journal of Archaeological Sciences 33, 14.
Richardson, M., Briggs, K., 2000. Seabed-Structure Interaction in Coastal Sediments. Office Navy Res. Rep., Arlington, VA, p. 18.
Saunders, R.D., 2005. Seabed Scour Emanating from Submerged Three-dimensional Objects: Archaeol. Case Studies, Dept Civil and Environmental Engineering University of Southampton, UK, p. 207.
Schrottke, K., Becker, M., Bartholomä, A., Flemming, B., Hebbeln, D., 2006. Fluid mud dynamics in the Weser estuary turbidity zone tracked by high-resolution side-scan sonar and parametric sub-bottom profiler. Geo-Marine Letters 26, 185-198.
Traykovski, P., Geyer, R., Sommerfield, C., 2004. Rapid sediment deposition and fine-scale strata formation in the Hudson estuary. Journal of Geophysical Research 109, 20.
Traykovski, P., Richardson, M.D., Mayer, L.A., Irish, J.D., 2007. Mine Burial Experiments at the Martha's Vineyard coastal observatory. Oceanic Engineering, IEEE Journal
32, 150-166.
Trembanis, A.C., Friedrichs, C.T., Richardson, M.D., Traykovski, P., Howd, P.A., Elmore, P.A., Wever, T.F., 2007. Predicting Seabed Burial of Cylinders by Wave-Induced Scour: Application to the Sandy Inner Shelf Off Florida and Massachusetts. Oceanic Engineering, IEEE Journal 32, 167-183.
Uncles, R.J., Stephens, J.A., Law, D.J., 2006. Turbidity maximum in the macrotidal, highly turbid Humber Estuary, UK: Flocs, fluid mud, stationary suspensions and tidal bores. Estuarine Coastal Shelf Sciences 67, 30-52.
Velasco, D.W., Huhta, C.A., 2010. Experimental verification of acoustic Doppler velocimeter (ADV) performance in fine-grained, high sediment concentration fluids, SonTek/YSI Appl. Note.
Verfaillie, E., Meirvenne, M.V., Lancker, V.V., 2006. Multivariate geostatistics for the predictive modelling of the surficial sand distribution in shelf seas. Continental Shelf Research 26, 15.
Voropayev, S.I., Testik, F.Y., Fernando, H.J.S., Boyer, D.L., 2003. Burial and scour around short cylinder under progressive shoaling waves. Oceanic Engineering 30, 1647-1667.
Wever, T., 2003. Speed of Migrating Bedforms on the Sea Floor - A Review, FWG-Report. Forschungsanstalt der Bundeswehr für Wasserschall und Geophysik, pp. 20.
Wever, T.F., Luehder, R., 2007. Mine Burial Observations During the 2003-2004 U.S. Office of Naval Research Experiment. Oceanic Engineering, IEEE Journal 32, 184-190.
Wilkens, R.H., Richardson, M.D., 2007. Mine Burial Prediction: A Short History and Introduction. Oceanic Engineering, IEEE Journal 32, 3-9.
Winterwerp, J.C., 2002. On the flocculation and settling velocity of estuarine mud. Continental Shelf Research 22, 1339-1360.
Yang, L., 1998. Modelling of hydrodynamic processes in the Belgian Coastal Zone, Appl. Math. Catholic University of Louvain, Leuven, p. 204.